



Two islands, one ray: Age and growth pattern of the common eagle ray (*Myliobatis aquila*) in the Central Mediterranean (Sicily and Sardinia)

Andrea Bellodi^{a,b,1}, Manfredi Madia^{b,e,*}, Blondine Agus^a, Pierluigi Carbonara^c,
Massimiliano Bottaro^d, Mauro Sinopoli^{e,2}, Maria Cristina Follesa^{b,2}

^a Department of Integrated Marine Ecology, Calabria Marine Center, Stazione Zoologica Anton Dohrn (SZN), C. da Torre Spaccata, Località Torre Spaccata, Amendolara 87071, Italy

^b Department of Life and Environmental Sciences, University of Cagliari, Cagliari 09126, Italy

^c Fondazione COISPA ETS, Via dei Trulli 18/20, Bari 70126, Italy

^d Department of Integrative Marine Ecology, Genoa Marine Centre, Anton Dohrn Zoological Station, Genoa 16126, Italy

^e Stazione Zoologica Anton Dohrn, (National Institute of Biology, Ecology and Marine Biotechnology), Sicily Marine Centre, Department of Integrative Marine Ecology, Palermo, Italy

ARTICLE INFO

Keywords:

Myliobatiformes
Multi-model inference analysis
Bayesian growth modelling
Vertebral Centra
Back-calculation

ABSTRACT

The common eagle ray represents one of the most threatened batoid species inhabiting the Mediterranean Sea. Despite its low commercial value, the species is frequently encountered in both commercial and artisanal fishery bycatch. Nonetheless, the information available on its life history, especially its growth pattern, are rather scarce. Given the importance of growth data for accurately assessing the status of a species' population and informing its management, this study aims to provide new insights into the growth patterns of the common eagle ray in the western-central Mediterranean Sea. Between 2014 and 2024 a total of 200 vertebral centra were analysed from specimens caught along the coast of the two major Mediterranean islands (Sicily and Sardinia). Vertebrae were only extracted from specimens that were found to be already dead at the time of the capture, while live individuals have been released. To accurately describe the species' growth, different models were fitted to age-at-length data in a multi-model inference analysis. The von Bertalanffy growth function was indicated by the corrected Akaike's Information Criterion as the most accurate in describing the species' growth. Results indicated that females reaching larger sizes (in disk width, DW) and greater longevity (DW: 189–737 mm; age range: 0–10 years) but growing at a slower rate ($DW_{\infty} = 872.9$ mm; $k = 0.11$ y^{-1} ; $t_0 = -2.36$) compared to males, which showed smaller maximum sizes and shorter lifespans (DW: 250–567 mm; age range: 0–7 years; $DW_{\infty} = 511.1$ mm; $k = 0.36$ y^{-1} ; $t_0 = -1.36$).

1. Introduction

Elasmobranchs, although often considered charismatic and symbolically important species in many cultures, constitute a significant component of both professional and artisanal fishery bycatch (Stevens et al., 2000; Ellis et al., 2017). Due to their high susceptibility to anthropogenic disturbances, particularly fishing activity, a huge number of sharks' and rays' stocks worldwide are facing a sharp decline in recent years (White et al., 2012; Ellis et al., 2017; Dulvy et al., 2021; Pacoureau et al., 2021). However, the biological information required for effective management of these species is frequently incomplete or entirely lacking

(Porcu et al., 2020). This lack of knowledge is especially pronounced for rare or less common taxa, which are therefore often among the most threatened.

Among the life-history parameters needed for proper assessment, growth information is fundamental to understanding population dynamics and resilience (Campana, 2014). However, modelling Elasmobranchs' growth has often been considered a more challenging process than for bony fish, due to the otoliths' absence and the low calcification level of the structures used as an alternative (Goldman et al., 2012), together with the usually higher difficulty in gathering a sufficient sample size for rare or threatened species (Smart et al., 2013). The

* Corresponding author at: Department of Life and Environmental Sciences, University of Cagliari, Cagliari 09126, Italy.

E-mail address: manfredi.madia@unica.it (M. Madia).

¹ Equally contributing first authors

² joint last authors

situation described above perfectly fits to the common eagle ray (*Myliobatis aquila* Linnaeus, 1758), a benthopelagic batoid species belonging to the family Myliobatidae.

M. aquila, commonly known as the common eagle ray, is a benthic–demersal batoid widely distributed in the eastern Atlantic Ocean and throughout the Mediterranean Sea. The species inhabits coastal and shelf waters, where it is typically associated with sandy and muddy substrates, and feeds primarily on benthic invertebrates (CIESM, 2023; Serena, 2005). Despite its wide range, biological information on *M. aquila* remains limited, particularly with respect to age, growth, and population-specific life-history traits.

The geographical distribution of *M. aquila* spans the eastern Atlantic, from the British Isles and the North Sea to South Africa, including the entire Mediterranean basin, where it is the sole representative of its genus (Whitehead et al., 1986). In Italian waters, it occurs along all coasts, typically between 50 and 200 m depth, where fine sediments and organic detritus facilitate benthic foraging (Vacchi and Serena, 2010).

Despite lacking direct commercial value, *M. aquila* is frequently captured as bycatch in trawl nets, gillnets, and bottom longlines, contributing to significant population declines in Italian and wider Mediterranean waters (Madia et al., 2024). Moreover, estimates based on official records and unreported landings indicate that the Mediterranean population has declined by over 50% in the past forty years. This situation is likely exacerbated by underreporting in countries with less stringent catch monitoring (La Mesa et al., 2016). The IUCN classifies *M. aquila* as "Vulnerable" in European and Mediterranean waters (Malak et al., 2011) and more recently as Critically Endangered on a global scale due to new data indicating severe declines outside the Mediterranean (Jabado et al., 2021).

Given the high conservation concern associated with this species, it is essential to obtain robust estimates of key life-history parameters, such as age at maturity, growth rate, longevity, and age-class structure, to evaluate population resilience and to support both fisheries management and conservation planning (Cortés, 2002; Natanson et al., 2006). Detailed quantitative data for *M. aquila* in the whole Mediterranean Sea still remain scarce, with only a few available studies in the western area of the basin and in the Adriatic Sea, mostly regarding its feeding ecology (Jardas et al., 2004; Valls et al., 2011; Lipej et al., 2025), general biology (Rafrafi-Nouira et al., 2017), distribution and presence in by-catch (La Mesa et al., 2016; Bonanomi et al., 2018a) and length-weight relationship (Colombelli and Bonanomi, 2022). Moreover, in the Eastern Mediterranean additional contributions mainly address length–weight relationships (Filiz and Bilge, 2004; Ismen et al., 2007; Ilkyaz et al., 2008; Yiğın and İsmen, 2009; Cabbar and Yiğın, 2021), trophic ecology (Gül & Demirel, 2020), and bycatch composition (Ceyhan et al., 2010; Keskin et al., 2014; Bengil and Başusta, 2018).

Despite the species' conservation importance, only one study has provided growth data a recent analysis from Turkish waters (Özten et al., 2024). This contribution and, in general, many studies on growth parameters for batoids have traditionally relied on the von Bertalanffy function, which remains widely used for fish species (Liu et al., 2021). However, recent analyses on chondrichthyans' growth have increasingly emphasized the benefit of using a multiple growth models approach comparing alternative sigmoidal models (e.g. Gompertz, Logistic) to capture potential species-specific growth dynamics more effectively (e.g. Liu et al., 2021; Bellodi et al., 2022). These data will provide a robust foundation for developing population dynamic models, informing future conservation assessments, and supporting targeted management measures aimed at ensuring the conservation of this important species. This study, therefore aims to fill current knowledge gaps through a comparative multi-model growth analysis, conducted through both a traditional frequentist and a Bayesian approach, based on specimens collected from the two largest Mediterranean islands, Sicily and Sardinia. The data presented here will provide the first regional growth estimates for this threatened species, establishing a quantitative basis for future population-dynamic modelling and risk

assessment approaches.

2. Material and methods

2.1. Sample composition

Between 2014 and 2024, specimens of *M. aquila* were collected through two main sources: i) Commercial fishing monitoring conducted in ports along the western coast of Sicily between 2023 and 2024; ii) The Mediterranean International Trawl Survey (MEDITS; AAVV, 2017), which provided samples from Sardinian waters between 2014 and 2018 (Fig. 1). Given the threatened status of *M. aquila* populations, only specimens that were found dead upon capture were retained and used for this study, while individuals that were still alive were released, following all best practices for the proper handling of cartilaginous fish by-catch (Carpentieri et al., 2021).

For each specimen found to be dead at the capture in the sampling period, the disc width (DW, mm), defined as the maximum straight-line distance between the tips of the pectoral fins and the sex were recorded and a portion of the vertebral column was extracted. To evaluate potential sampling biases, we tested the geographic and temporal distribution of specimens across sampling areas and months using chi-square goodness-of-fit tests. Potential spatial and seasonal biases in growth-related traits were assessed by testing differences in DW among areas and sampling months using a non-parametric Kruskal–Wallis test. Disk width was selected as a key morphometric variable directly related to individual growth. In addition, a bootstrap sensitivity analysis (1000 iterations) was conducted to assess the robustness of DW estimates to sampling variability within the observed dataset. Additionally, in order to investigate the potential influence of seasonal bias, an additional sensitivity analysis was run by excluding summer samples (June–September) and re-evaluating DW distributions. All this analysis were conducted in R (ver. 4.5.2; R Core Team, 2026).

2.2. Vertebral centra extraction and sectioning

From each specimen, approximately 10 vertebrae were extracted from the abdominal cavity region (immediately posterior to the scapular origin of the vertebral column), where the vertebral centra are bigger and thus easier to analyse (Campana, 2014; Bellodi et al., 2017b, 2019). Prior age analysis, the vertebrae were stored at -20°C . Subsequently, the vertebral centra were defrosted, soft tissues (muscle, skin, and neural material) were removed by immersion in a 5% sodium hypochlorite solution (Goldman, 2006; Bellodi et al., 2017b; Porcu et al., 2020), and the neural and hematic arches were removed with a scalpel. The centra were then measured considering the vertebral length (VL) and vertebral diameter (VD) to the nearest 0.1 mm (Goldman, 2006) and then embedded in epoxy resin (QATM Kem 90). From each embedded centra thin sections (~ 0.8 mm) were cut with a cutting machine (IsoMet 1000) with a circular diamond blade (Bellodi et al., 2019; Porcu et al., 2020). If necessary, they were thinned to increase their readability by grinding with a polisher (QATM Qpol 250M1) (grit 800). The sections' final width ranged between 0.3 and 0.5 mm. In order to be examined, sections were then immersed in a clarification medium (seawater) and photographed under a stereomicroscope (NSZ-818) equipped with a high-resolution camera (CNOPTec CA812) using reflected light against a black background. The length of the *corpus calcareum* (CCL) and the distance from the vertebra center to each transparent band (B1, B2, ..., Bn) were measured (Fig. 2) using the ImageJ software (ImageJ, National Institutes of Health, USA).

2.3. Age estimation, reading precision and growth modelling

Ages were determined by counting alternating translucent and opaque bands, each pair representing one annulus (Sulikowski et al., 2003). Translucent bands were counted starting from the first translucent band

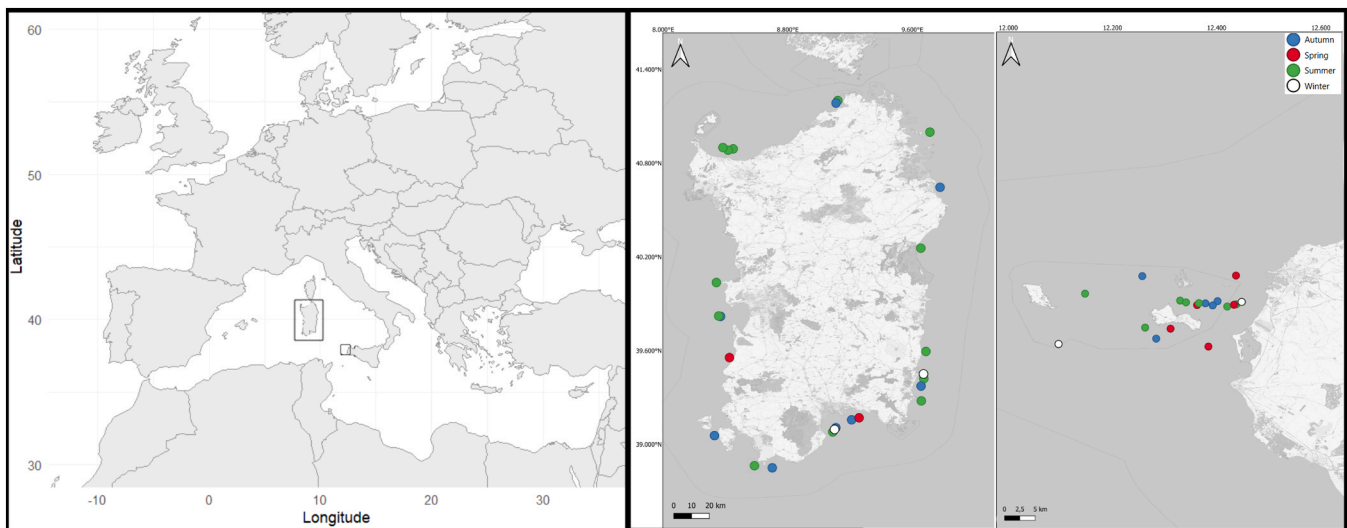


Fig. 1. *Myliobatis aquila* sampling areas with indications of sampling sites per month.

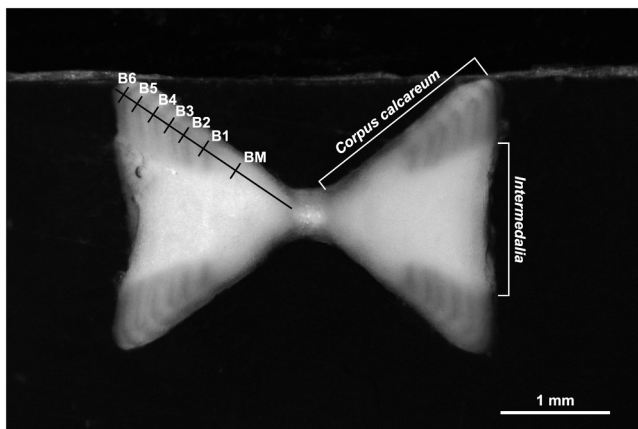


Fig. 2. Growth pattern interpretation and definition of the measurement taken on a *Myliobatis aquila* sectioned vertebral centra (Male, 440 mm DL). BM indicates the birthmark and B1, B2... B6 are respectively the distance from the centra focus of the 1st, 2nd, 6th winter bands.

clearly visible after the birthmark (BM) was identified as the first clear mark corresponding to a change of angle in the CCL shape (Sulikowski et al., 2003) (Fig. 2). The nature of the vertebral edge (translucent or opaque) was also recorded. The pattern of annulus deposition on the vertebrae was analyzed by a semi-direct qualitative marginal analysis approach (Campana, 2001, 2014) and the annual periodicity of band deposition was evaluated following the criteria described by Okamura and Semba (2009). The marginal analysis considered the monthly evolution of the edge types (transparent or opaque) of the hard structures. The two edge types were defined when over 75% of the corpus calcareum margin appeared transparent or opaque. Vertebral sections in which about 50% of the edge was opaque or transparent were not included in the analysis (Carbonara et al., 2018). The age was assigned to each vertebral section according to the ageing scheme proposed by Carbonara and Follasa (2019) with a yearly resolution, with the birthday set at January 1st. Each section's age was independently estimated by two experienced readers blinded to the specimen's sex and size. Readings were repeated up to three times per reader; vertebrae without consensus were discarded as unreadable. The reading precision and the inter-reader agreement were evaluated by the coefficient of variation (% CV) and percentage of agreement (PA) (Eltink, 2000) Precision and inter-reader agreement were evaluated using: i) Coefficient of Variation

(CV%) (Eltink, 2000); ii) Percentage Agreement (PA) (Eltink, 2000); iii) Index of Average Percent Error (IAPE) (Beamish and Fournier, 1981).

2.4. Growth modelling

Age-length data were fitted to four standard growth models using a frequentist approach:

- the common von Bertalanffy growth function with t_0 formulation (vb_ t_0) (von Bertalanffy, 1938); $DW = DW_{\infty}(1 - e^{-k(t-t_0)})$,
- the von Bertalanffy function with DW_0 formulation (vb_ L_0) (Fabens, 1965); $DW = DW_{\infty} - (DW_{\infty} - DW_0)e^{-kt}$,
- the Gompertz sigmoid curve (Gom) (Winsor, 1932); $DW = DW_{\infty} (e^{e^{-k(t-I)}})$,
- logistic curve (Logi) (Richards, 1959); $DW = DW_{\infty}/(1 + e^{-k(t-I)})$,

where DW_{∞} is the species' theoretical maximum length, k is the growth coefficient, t is the observed age, t_0 is the hypothetical disc width of a specimen at time 0, DW_0 is the known size at birth for the species (190 mm; Whitehead et al., 1986, Last et al., 2016), and I is the age at the curve inflection point. Growth modelling was performed through the R packages FSA and FSAdata (ver. 0.9.5 and ver. 0.4.1, respectively, Ogle et al., 2019).

Growth model's fitness for the collected age data was evaluated by the Akaike's information criterion (AIC; Akaike, 1974; Haddon, 2001) and the second order corrected Akaike's information criterion (AICc; Burnham and Anderson, 2002) calculated through the AICcmodavg R package (ver. 2.3-3, Mazerolle, 2020).

Differences between male and female growth were tested by comparing sex-specific and pooled best-fitting growth models using a likelihood ratio test following Kimura (1980).

Additionally, a back-calculation process was performed as suggested in Smart et al. (2013). On the basis of the obtained relationships between the TL and morphological measurements of vertebral centra (VL, VD, and CCL), the fish lengths at which different transparent bands were deposited were calculated using the back-calculation method. Distances from the vertebral centrum focus to each translucent band were measured on high-resolution images using image analysis software (ImageJ, National Institutes of Health, USA) The linear-modified Dahl-Lea method (Francis, 1990) was applied with the following formula:

$$L_i = L_c \times [(a+b \times CC_i)/(a+b \times CC_c)]$$

where a and b are the linear fit parameter estimates, L_i is the length at ring i , L_c is the length at capture, CC_c is the corpus calcareum.

The agreement between direct and back-calculated age estimates was assessed using Pearson correlation, Lin's concordance correlation coefficient (CCC), Bland–Altman analysis, and deming regression to test for additive and proportional bias. Back-calculated age-at-length data were used to estimate growth only for the model that provided the best fit to the observed data (based on AICc values) in order to increase the effective sample size and amend possible underrepresentation of certain size classes. Finally, in order to avoid potential bias due to uneven sampling, which often affect rare elasmobranch species such as *M. aquila*, a Markov Chain Monte Carlo (MCMC) growth estimation was used to extend multi-model growth estimation in a Bayesian approach (Smart and Grammer, 2021). These analyses were conducted in R environment using the BayesGrowth (ver. 1.0.0; Smart, 2023) and bayesplot (ver. 1.15.0, Gabry and Mahr, 2025) packages. Bayesian analysis worked on von Bertalanffy, Gompertz and logistic models with DW_0 formulation (Smart and Grammer, 2021). Both DW_0 and DW_∞ were considered as informative priors (including a 10% s.e.); these values were set considering known DW at birth (190 mm; Whitehead et al., 1986, Last et al., 2016) and maximum reported DW in the Mediterranean (1140 mm, Capapé et al., 2007) in all models (Smart and Grammer, 2021). Specifically, normal prior distributions were assigned to asymptotic size ($DW_\infty \sim \text{Normal}(1140, 114^2)$) and size at birth ($DW_0 \sim \text{Normal}(190, 4.85^2)$), while uniform priors were specified for the growth coefficient ($k \sim \text{Uniform}(0, 1)$) and residual error ($\sigma \sim \text{Uniform}(0, 100)$). To ensure that prior assumptions did not unduly influence posterior estimates, a prior sensitivity check was conducted by testing alternative, less informative prior specifications. The MCMC procedure was run with four independent chains, each with 10,000 iterations, a burn-in of 1000 iterations, and a thinning rate of 10. Convergence was assessed using the Gelman–Rubin diagnostic ($R < 1.1$ for all parameters), effective sample sizes, and visual inspection of trace and autocorrelation plots. In the Bayesian analysis, growth models were fitted using the DW_0 parameterization, as implemented in the BayesGrowth package, which requires the incorporation size at birth as biologically informative prior. Accordingly, three candidate models (von Bertalanffy with DW_0 formulation, Gompertz, and logistic) were evaluated, without including a t_0 -based formulation. Best model selection in the Bayesian framework was performed through the leave-one-out-cross-validation (LOOCV) where the best performing model accuracy is indicated by lower leave-one-out-information-criterion (LOOIC) and higher LOOIC weight (LOOICw). LOOCV analysis was carried out using the rstan (ver. 2.32.7; Stan Development Team, 2025) and loo (ver. 2.9.0; Vehtari, et al., 2025) R packages. A post hoc power analysis was conducted to evaluate the ability of the dataset to detect differences in DW between sexes and sampling areas, based on observed effect sizes (Cohen's d) and sample sizes. Statistical power was estimated using two-sample t -test approximations implemented in the R package *pwr* (ver. 1.3.0; Champely, 2020). Sex-specific differences in growth parameters were assessed by comparing posterior distributions obtained from separate Bayesian models fitted for males and females. Differences were quantified by estimating the probability of directional differences between sexes (i.e., the probability that a parameter from one sex exceeds that of the other) based on posterior samples, rather than relying solely on overlap of credible intervals.

3. Results

3.1. Sample composition

A total of 101 specimens (ranging from 274 to 737 mm DW), and 99 specimens (ranging from 172 to 584 mm) were sampled in Sicilian and Sardinian coasts, respectively. The distribution in sizes of the Sicilian population revealed a modal size class between 400 and 500 mm, with a progressive decline in frequency beyond this range. The highest

recorded DW was 737 mm, indicating the presence of large individuals (Fig. 3).

The Sardinian population displayed a different pattern, with the majority of individuals clustered between 300 and 400 mm. A few larger individuals were also present, but the size distribution showed a more restricted range compared to the Sicilian one (Fig. 3). Specific information on sample composition is reported in Table 1.

No significant geographic bias was detected in the distribution of sampled specimens between the two sampling areas ($\chi^2 = 0.24$, $p = 0.62$). Conversely, the temporal distribution of samples differed significantly from a uniform distribution across months ($\chi^2 = 99.25$, $p < 0.001$), indicating a marked seasonal bias in sampling, with a higher number of specimens collected during summer months. Specimens' DW differed significantly both between sampling areas (Kruskal–Wallis $\chi^2 = 63.78$, $p < 0.001$) and sampling months (Kruskal–Wallis $\chi^2 = 58.74$, $p < 0.001$). Finally, the bootstrap sensitivity analysis indicated stable estimates of mean DW (mean = 393.5 mm; 95% CI = 379.7–407.1 mm), suggesting robustness of central tendency estimates despite sampling heterogeneity. To further assess the influence of seasonal bias, an additional sensitivity analysis was performed excluding summer samples (June–September). A significant deviation from uniform monthly distribution persisted in the reduced dataset ($\chi^2 = 28.11$, $p < 0.001$), confirming uneven temporal sampling even after seasonal exclusion. However, this resulted in only a marginal change in mean DW (391.2 mm; $\Delta = -0.57\%$), with largely overlapping bootstrap confidence intervals (95% CI = 370.2–413.0 mm), indicating that seasonal bias had a limited effect on the overall size structure of the sampled population.

3.2. Age estimation, reading precision and growth modelling

Correlation and regression analyses between vertebral measurements (VL, VD, CCL) and DW emerged to be highly significant, equation parameters and detailed test results are reported in Supp. Table 1.

The aggregated results of IAPE (4.37%), CV (6.50%), and PA (89.1%) demonstrated great reading precision and consistency across all modal ages (Supp. Fig. 1). Furthermore, no evidence of bias among readers was found (bias test, Wilcoxon's matched-pairs signed rank test $z = -0.869$; $p > 0.05$).

The edge analysis revealed a very distinct deposition pattern for the annual growth bands. Model selection based on AIC strongly supported the annual model (AIC = 43.04; Akaike weight = 1.00), whereas both the non-cyclic and biannual models showed substantially lower support (AIC > 70), confirming an annual periodicity in growth band deposition, with opaque bands forming predominantly during the winter months (December to March) and translucent bands during the summer (May to September) (Fig. 4; Supp. Table 2 and Supp. Fig. 2).

Female specimens of the common eagle ray showed maximum ages. The oldest female was estimated to be 10 years old, while the oldest male was 7. The growth modelling based on the frequentist approach indicated the von Bertalanffy model as the one that appeared to be the most precise in terms of fitting to the observed data in all investigated scenarios. Indeed, for females, males and combined sexes of both the entire sample (Fig. 5A) and Sardinian population (Fig. 5B), the VB model always achieved the lower AICc values (Table 2). Females achieved higher DW_∞ values than males, which, on the other hand, showed higher growth rates (k) (Table 2; Fig. 5A,B). A likelihood ratio test comparing sex-specific and pooled von Bertalanffy growth models revealed significant differences between males and females ($\chi^2 = 29.40$, $df = 3$, $p < 0.001$) on the entire sample, indicating sex-related divergence in growth parameters. Unfortunately, the sample composition in sizes, with few age 0 specimens, did not allow for the growth modelling of the Sicilian population based on direct age estimation. For this reason, the analysis of this sample was carried out exclusively with back-calculated data (Table 2; Fig. 5C). Direct and back-calculated age estimates were strongly correlated in both Sardinia (Pearson correlation

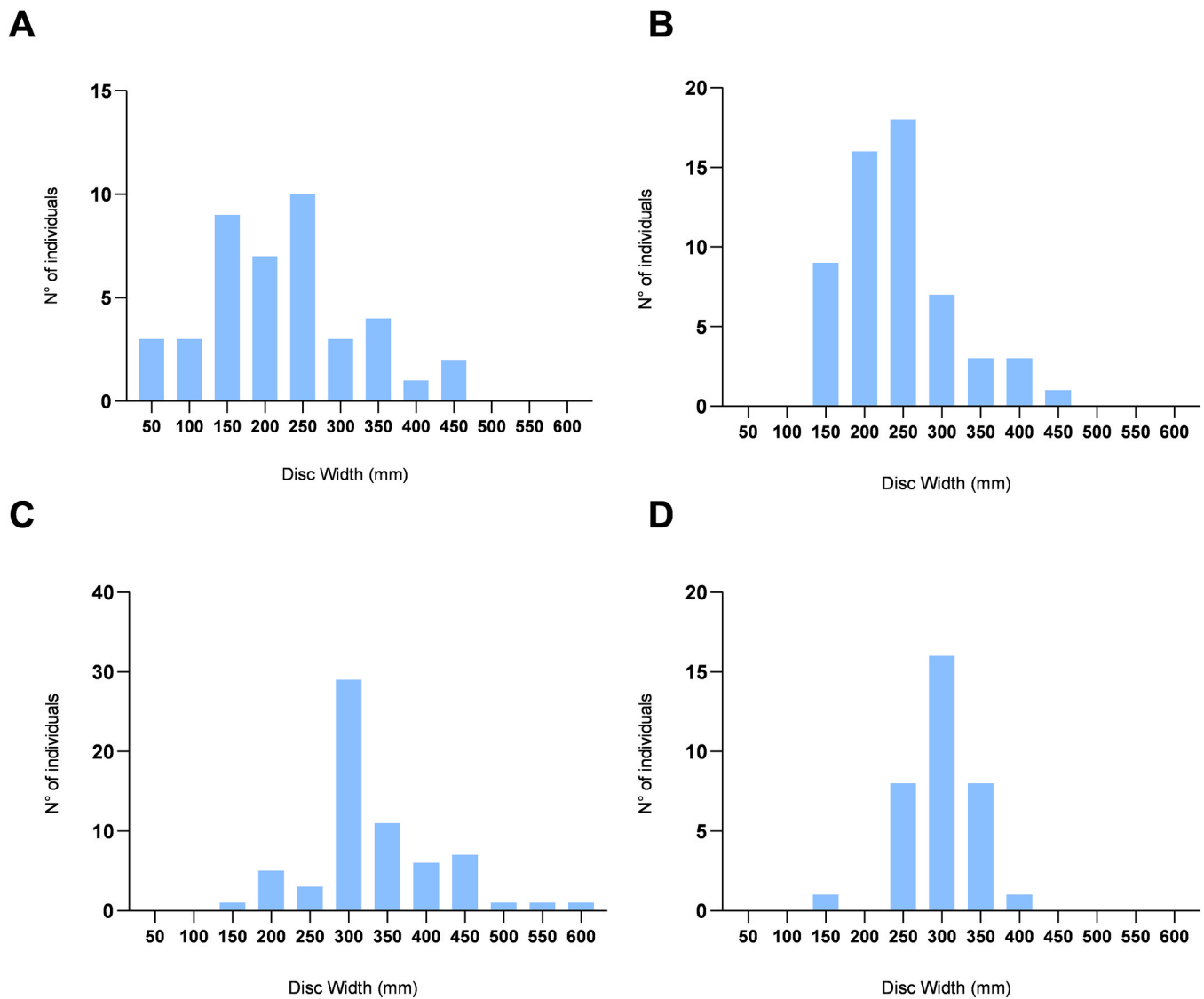


Fig. 3. Frequency distribution of *Myliobatis aquila* individuals by size class (disc width, DW) in 50 mm intervals, separated by sex and geographic area. Panel (A) females from Sardinia (B) males from Sardinia (C) females from Sicily (D) males from Sicily. The x-axis represents disc width size classes (mm), while the y-axis indicates the number of individuals within each class.

Table 1

Sample size (N), mean disc width (DW) ± standard deviation (SD), and size range (in mm) of *Myliobatis aquila* individuals by sex and geographic area.

Area	Sex	N	DW Mean ± SD	Range (mm)
Sardinia	Female	42	346.9 ± 97.9	189–584
	Male	57	362.5 ± 70.3	250–567
Sicily	Female	66	455.6 ± 80.0	295–737
	Male	35	419.9 ± 43.6	274–500

$p < 0.001$, $r = 0.939$) and Sicily (Pearson correlation $p < 0.001$, $r = 0.935$). These results appeared to be further confirmed by Lin’s CCC values, which indicated high agreement (Sardinia CCC = 0.904, Sicily CCC = 0.909).

Furthermore, the deming regression analysis revealed no significant proportional bias in the Sardinian sample (slope = 0.96, 95% CI: 0.87–1.05) and no additive bias (intercept = 0.49). In contrast, a slight proportional bias was detected in the Sicilian sample (slope = 1.13, 95% CI: 1.02–1.21).

The measurement of winter bands distances from the vertebral focus seemed to follow a similar path both in the Sicilian and Sardinian sample

(Fig. 6). The VB parameters obtained from back-calculated age-at-length data are also reported in Table 2.

Confirming what emerged through the frequentist growth modelling, the MCMC growth analysis results indicated von Bertalanffy’s model as the most accurate in terms of the observed data (lower LOOIC and higher LOOICw values) both for the entire sample and the two areas separately (Table 3). The von Bertalanffy growth curves estimated with the bayesian approach for the entire sample and for Sardinia and Sicily separately are showed in Fig. 5E, F and G, respectively. Model diagnostic analysis (MCMC chain convergence and parameters’ autocorrelation) showed optimal results for every parameter considered for each model, suggesting high analysis reliability. The MCMC chain convergence and parameters autocorrelation plots for the best-fitting model (vb) are reported in Figs. 7 and 8, respectively. Trace plots (Fig. 7) revealed stable and well-mixed chains with no apparent trends or divergences among iterations, while autocorrelation plots (Fig. 8) showed a rapid decay, indicating low serial dependence between samples. All parameters exhibited R values close to 1 and high effective sample sizes, confirming proper convergence and reliability of posterior estimates. Although the von Bertalanffy growth parameters estimated for the entire sample using the MCMC approach were similar to those obtained with the frequentist

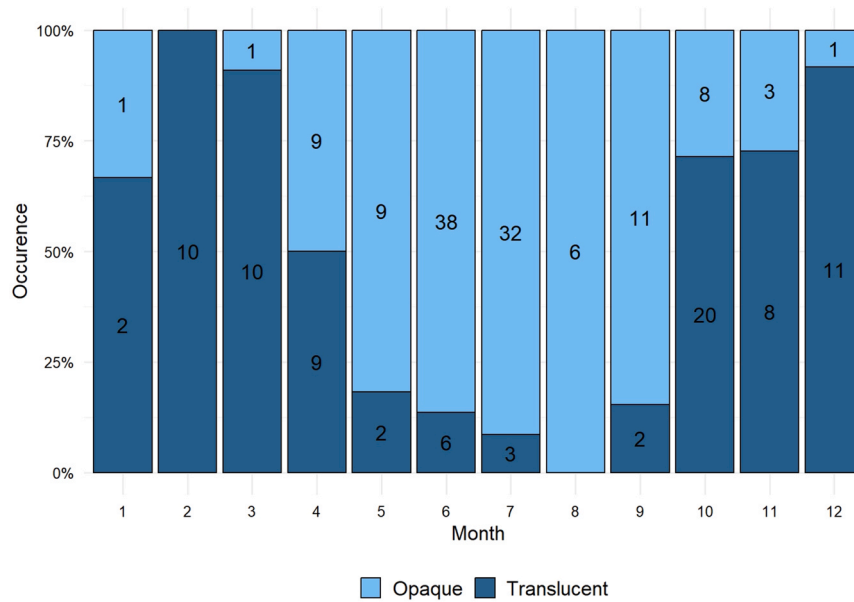


Fig. 4. *Myliobatis aquila* annual deposition pattern of translucent and opaque growth bands.

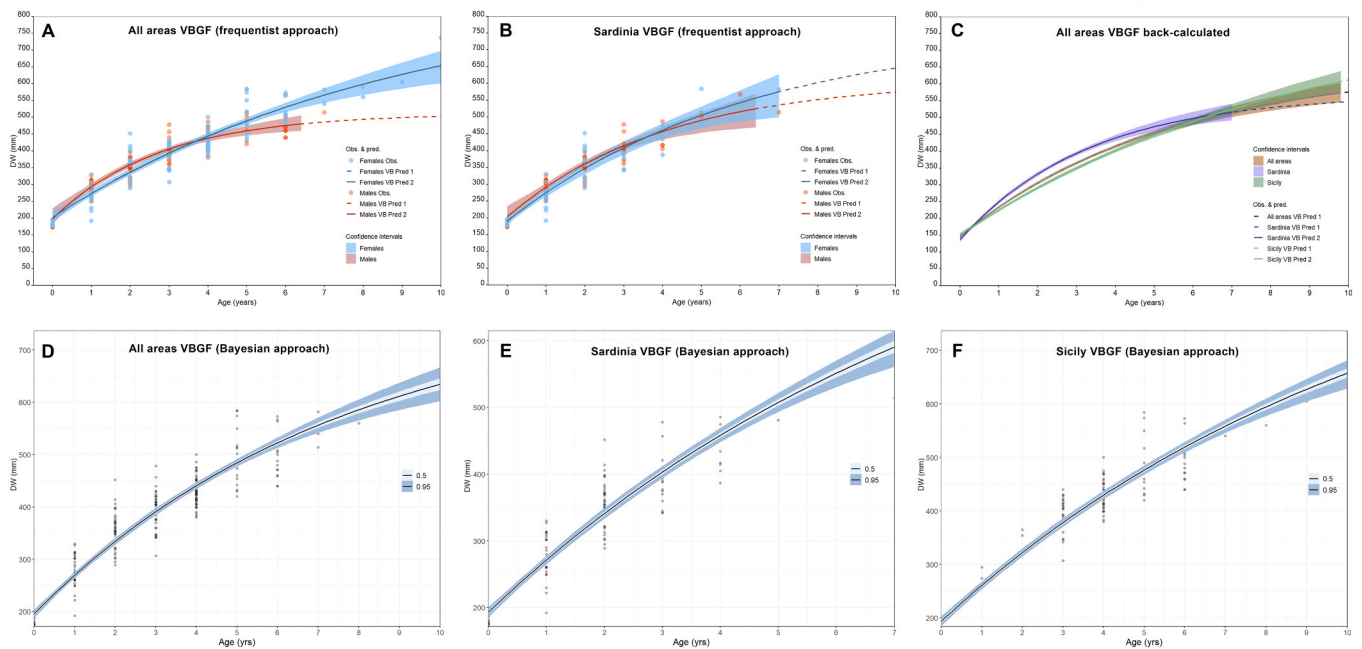


Fig. 5. *Myliobatis aquila* von Bertalanffy growth curves based on frequentist approach for the entire sample (A) and Sardinian (B) females and males; and the back-calculated von Bertalanffy curves of Sicilian, Sardinian and the entire sample (sexes combined) (C). Figures D, E and F show the Bertalanffy growth curves based on the Markov Chain Monte Carlo (MCMC) Bayesian approach estimated for the entire, the Sardinian and the Sicilian samples, respectively.

method, the Bayesian approach yielded a markedly higher DW_{∞} and a lower growth rate compared to the frequentist estimates when each area was analyzed separately (Tables 2 and 3).

The power analysis based exclusively on DW highlighted the presence of low statistical power for detecting differences between sexes (Cohen’s $d = 0.27$; power = 0.49), suggesting that this metric alone may have limited sensitivity in detecting sexual dimorphism. In contrast, the same analysis showed high differences between sampling areas (Cohen’s $d = 1.27$; power = 1.00). However, despite the limited power based on DW alone, both frequentist and Bayesian analyses of growth parameters revealed clear and consistent sexual dimorphism, supported by strong separation of posterior distributions ($P \approx 1.00$). In fact, similarly to

what emerged with the frequentist approach, Bayesian posterior distributions of growth parameters revealed marked sex-specific differences (Females \pm se: $DW_{\infty} = 1009.69 \pm 1.59$, $k = 0.09 \pm 0.01$, $DW_0 = 192.60 \pm 0.07$, $\sigma = 39.38 \pm 0.05$; Males \pm se: $DW_{\infty} = 545.77 \pm 0.53$, $k = 0.30 \pm 0.04$, $DW_0 = 190.43 \pm 0.08$, $\sigma = 30.29 \pm 0.04$). Asymptotic size (DW_{∞}) showed no overlap between sexes, with females consistently reaching larger sizes than males ($P \approx 1.00$). Conversely, males exhibited higher growth coefficients (k) than females ($P \approx 1.00$), indicating faster growth toward a smaller asymptotic size. These results provide strong evidence of sexual dimorphism in growth patterns. Overall, Bayesian estimates were consistent with frequentist results when the full dataset was considered, with comparable DW_{∞} and k values. However,

Table 2

Myliobatis aquila growth parameters (mean ± S.D.) calculated through the frequentist approach from each investigated growth model and for von Bertalanffy's back-calculated (vb BK) for combined sexes and females and males separately. DW_{∞} = maximum asymptotic disc width; k = growth coefficient; t_0 = theoretical age at which size equals zero; I = Inflection Point; AIC = Akaike's Information Criterion; AICc = corrected Akaike's Information Criterion. Values of the best fitting model are highlighted in bold.

Area	Sex	Model	DW_{∞}	k	t_0	I	AIC	AICc
Entire sample	Combined	Vb_ t_0	747.03 ± 224.20	0.14 ± 0.06	-2.34 ± 0.72	-	2099.87	2100.07
		Vb_ L_0	664.87 ± 145.86	0.20 ± 0.07	-	-	2105.21	2105.33
		Gom	666.68 ± 195.01	0.10 ± 0.19	-	0.24 ± 0.39	2110.41	2110.60
		Logi	631.63 ± 126.69	0.24 ± 0.11	-	1.57 ± 1.20	2119.99	2120.19
		vb BK	694.32 ± 71.76	0.16 ± 0.04	-1.37 ± 0.17	-	-	-
	Females	vb_ t_0	872.94 ± 110.49	0.11 ± 0.06	-2.36 ± 0.71	-	1115.24	1115.63
		Vb_ L_0	809.84 ± 236.59	0.13 ± 0.06	-	-	1116.79	1117.02
		Gom	735.94 ± 164.23	0.21 ± 0.12	-	0.22 ± 0.07	1119.64	1120.03
		Logi	684.77 ± 132.15	0.34 ± 0.09	-	2.21 ± 1.21	1123.99	1123.38
		vb_ t_0	511.11 ± 73.50	0.36 ± 0.13	-1.36 ± 0.63	-	960.54	960.97
	Males	Vb_ L_0	503.08 ± 39.05	0.39 ± 0.08	-	-	961.18	961.43
		Gom	494.65 ± 46.31	0.14 ± 0.10	-	0.49 ± 0.15	963.71	964.14
		Logi	485.22 ± 39.46	0.63 ± 0.18	-	0.37 ± 0.25	966.78	967.21
		vb_ t_0	658.20 ± 173.18	0.21 ± 0.09	-1.67 ± 0.49	-	1095.52	1095.91
		Vb_ L_0	635.06 ± 118.49	0.23 ± 0.08	-	-	1097.11	1097.33
Sardinia	Combined	Gom	590.00 ± 98.13	0.07 ± 0.11	-	0.37 ± 0.13	1099.95	1100.33
		Logi	560.65 ± 86.10	0.52 ± 0.14	-	0.99 ± 0.49	1104.45	1104.83
		vb BK	598.13 ± 55.27	0.25 ± 0.06	-0.91 ± 0.13	-	-	-
		vb_ t_0	758.66 ± 179.81	0.16 ± 0.09	-1.79 ± 0.65	-	482.22	483.17
		Vb_ L_0	754.41 ± 780.93	0.16 ± 0.14	-	-	483.26	483.78
	Females	Gom	634.94 ± 218.14	0.07 ± 0.11	-	0.37 ± 0.13	483.73	484.68
		Logi	590.78 ± 152.41	0.50 ± 0.21	-	1.33 ± 1.14	485.57	486.52
		vb_ t_0	658.20 ± 169.33	0.24 ± 0.19	-1.65 ± 1.03	-	615.91	616.61
		Vb_ L_0	573.62 ± 110.36	0.30 ± 0.13	-	-	616.21	616.82
		Gom	565.84 ± 195.87	0.01 ± 0.17	-	0.38 ± 0.24	618.69	619.39
	Males	Logi	545.11 ± 127.27	0.53 ± 0.25	-	0.77 ± 0.97	621.18	621.89
		vb BK	815.57 ± 177.23	0.12 ± 0.04	-1.72 ± 0.27	-	-	-
		vb_ t_0	658.20 ± 173.18	0.21 ± 0.09	-1.67 ± 0.49	-	1095.52	1095.91
		Vb_ L_0	635.06 ± 118.49	0.23 ± 0.08	-	-	1097.11	1097.33
		Gom	590.00 ± 98.13	0.07 ± 0.11	-	0.37 ± 0.13	1099.95	1100.33
Sicily	Combined	Logi	560.65 ± 86.10	0.52 ± 0.14	-	0.99 ± 0.49	1104.45	1104.83
		vb BK	598.13 ± 55.27	0.25 ± 0.06	-0.91 ± 0.13	-	-	-
		vb_ t_0	758.66 ± 179.81	0.16 ± 0.09	-1.79 ± 0.65	-	482.22	483.17
		Vb_ L_0	754.41 ± 780.93	0.16 ± 0.14	-	-	483.26	483.78
		Gom	634.94 ± 218.14	0.07 ± 0.11	-	0.37 ± 0.13	483.73	484.68
	Females	Logi	590.78 ± 152.41	0.50 ± 0.21	-	1.33 ± 1.14	485.57	486.52
		vb_ t_0	658.20 ± 169.33	0.24 ± 0.19	-1.65 ± 1.03	-	615.91	616.61
		Vb_ L_0	573.62 ± 110.36	0.30 ± 0.13	-	-	616.21	616.82
		Gom	565.84 ± 195.87	0.01 ± 0.17	-	0.38 ± 0.24	618.69	619.39
		Logi	545.11 ± 127.27	0.53 ± 0.25	-	0.77 ± 0.97	621.18	621.89
	Males	vb BK	815.57 ± 177.23	0.12 ± 0.04	-1.72 ± 0.27	-	-	-

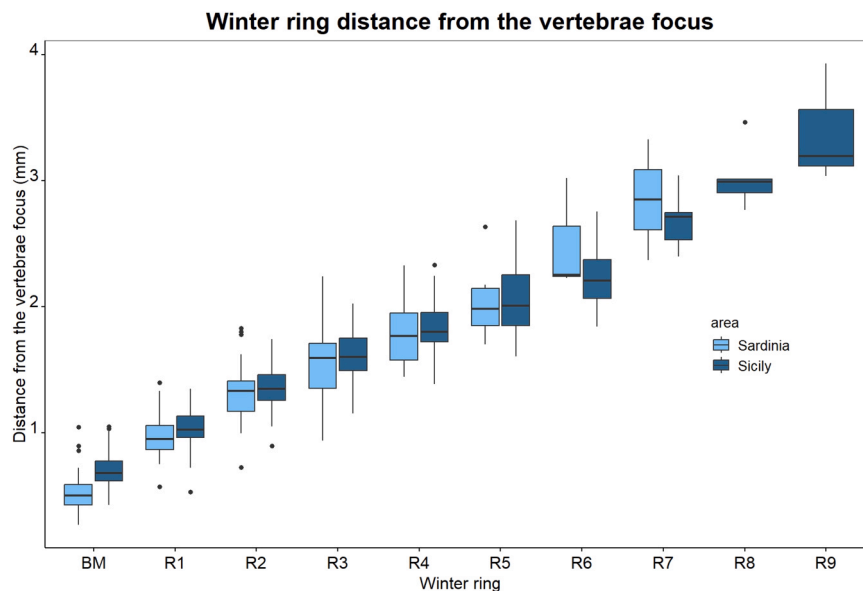


Fig. 6. Distance from the vertebral focus of the birthmark (BM) and each winter band (R1, R2,...Rn) of *Myliobatis aquila* sampled in Sicily and Sardinia. Specifically, the central horizontal line indicates the median; the box represents the interquartile range (IQR; 25th–75th percentiles); and the whiskers extend to the most extreme values within $1.5 \times$ IQR from the lower and upper quartiles. Observations beyond this range are plotted individually as outliers (shown as points).

confidence intervals tended to be wider than frequentist confidence intervals in area-specific analyses, reflecting increased uncertainty associated with reduced sample size and uneven size distribution.

4. Discussions

The entire age reading estimation protocol appeared to be a highly reliable process for *M. aquila*. The vertebral sections displayed well-defined banding patterns, with clear alternation between opaque and

translucent zones, together with an often-simple identification of the birthmark, allowed for reliable and reproducible readings. Therefore, the ageing precision indices (%CV, IAPE, PA) and the high inter-reader agreement obtained were fully consistent with the thresholds typically used in elasmobranch studies (Campana, 2014; ICES, 2011), confirming the robustness of the adopted protocol, as previously employed and validated in other Mediterranean ray species (e.g. Carbonara et al., 2020; Porcu et al., 2020). The confirmation of the annual periodicity of growth bands, with opaque bands deposited in winter and translucent

Table 3

Myliobatis aquila growth parameters (mean \pm S.D.) calculated through the Bayesian Markov Chain Monte Carlo (MCMC) approach from each investigated growth model for combined sexes. DW_{∞} = maximum asymptotic disc width; k = growth coefficient; DW_0 = disk width at birth; σ = normal residual error; LOOIC = leave-one-out information criterion; LOOICw = leave-one-out information criterion weight. Values of the best fitting model are highlighted in bold.

Area	Model	DW_{∞}	k	DW_0	σ	LOOIC	LOOICw
Entire sample	vb	804.64 \pm 70.25	0.13 \pm 0.02	195.56 \pm 4.31	37.59 \pm 1.91	2092.870	1.00
	Gom	647.06 \pm 30.86	0.29 \pm 0.03	198.03 \pm 4.23	38.77 \pm 1.97	2106.611	0.00
	Logi	596.01 \pm 20.32	0.44 \pm 0.03	200.73 \pm 4.18	40.21 \pm 2.01	2121.709	0.00
Sardinia	vb	929.90 \pm 118.48	0.12 \pm 0.03	192.89 \pm 4.05	36.09 \pm 2.57	1092.946	0.77
	Gom	652.77 \pm 57.50	0.32 \pm 0.04	193.43 \pm 4.33	36.39 \pm 2.67	1095.672	0.20
	Logi	576.66 \pm 30.15	0.53 \pm 0.05	194.29 \pm 4.23	37.04 \pm 2.64	1098.957	0.04
Sicily	vb	993.13 \pm 100.76	0.09 \pm 0.02	193.70 \pm 4.77	38.66 \pm 2.87	996.2662	0.99
	Gom	752.16 \pm 55.73	0.22 \pm 0.02	195.07 \pm 4.83	40.11 \pm 2.93	1005.1967	0.01
	Logi	659.23 \pm 33.54	0.38 \pm 0.03	195.94 \pm 4.83	41.37 \pm 3.08	1013.0980	0.00

bands in summer, aligns with observations from other Mediterranean batoid species (Sulikowski et al., 2003; Carbonara et al., 2020). The marginal analysis, although based on qualitative data, validated the assumption of annual band formation (sensu Okamura & Semba, 2009). Such indirect validation provides a reliable and practical framework for species where chemical tagging or controlled growth observations are not feasible.

The lack of small individuals, the samples' composition in size did not allow the frequentist growth modelling of Sicilian specimens using exclusively direct observation; therefore, for this area, the species growth was analysed only through back-calculated data. In this regard, when comparing back-calculation results it should be taken into account that although a minor proportional bias was detected for the Sicilian sample, the high CCC values and strong correlations indicate that back-calculated ages provide reliable estimates. Nonetheless, the presence of this potential bias, should be considered when interpreting regional growth comparisons. The absence of small individuals in the sample from Sicilian waters could be ascribed to the different sampling gear used in this area with respect to the one used in Sardinia. In fact, while common eagle rays in Sicily were collected as bycatch from artisanal trammel nets monitoring, Sardinian specimens were caught during the MED.I.T.S. scientific bottom trawl survey (Spedicato et al., 2019, see materials and methods), which, using a less selective gear in this survey allowed the capture of smaller specimens. Conversely, all the largest specimens observed ($DW > 450$ mm) were caught in the Sicilian area.

The multi-model inference analysis based on the frequentist approach conducted in this study on *M. aquila* identified the von Bertalanffy growth function (VBGF) as the most precise in terms of fitting to the observed age-at-length data, among the applied growth models with the lowest AICc values in all investigated scenarios (combined sexes, males, and females). This result appeared to be further confirmed by the Bayesian analysis, which also indicated the von Bertalanffy function as the most precise in describing the growth pattern of the common eagle ray across all considered scenarios. Recent literature (Liu et al., 2021) suggested that, for many batoid species, sigmoidal models may offer a more realistic description of early growth stages. However, this seems unlikely to be the case of *M. aquila*, whose growth seems to follow a more uniform pattern as suggested by the fact that the VBGF emerged as the best fitting model in both frequentist and Bayesian approaches. This result is consistent with findings from other batoid species in the central Mediterranean, such as *Raja clavata* (Carbonara et al., 2020, Bellodi et al., 2022).

To address the potential bias in growth modelling caused by sampling issues, which frequently impact uncommon and threatened elasmobranchs, we chose to use a Bayesian approach in addition to classical frequentist modelling in the current study. Interestingly, considering the entire sample the MCMC growth modelling returned von Bertalanffy's DW_{∞} and k values very similar to those obtained through the frequentist approach, indicating that the sample number and size distribution were probably sufficient to provide reliable growth estimations. Conversely, the Bayesian approach yielded higher DW_{∞} and lower k values than the

frequentist estimation when the two investigated areas were analyzed separately. This implies that, as previously mentioned, potential biases may exist as a result of an unbalanced size distribution or a small sample size when the two areas are examined separately. These findings emphasize the need of implementing a Bayesian technique in addition to conventional frequentist analysis when working with rare elasmobranch species, which frequently do not allow for optimal sampling (Smart and Grammer, 2021). In this context, the Bayesian approach seemed to be able to provide additional inferential value beyond traditional frequentist approaches. Incorporating prior biological knowledge and generating full posterior distributions, it allowed a more comprehensive quantification of uncertainty in growth parameters. This is particularly relevant for rare and threatened species, where limited and unbalanced samples may bias parameter estimation (Smart and Grammer, 2021). Therefore, the integration of Bayesian and frequentist approaches appears to represent a complementary strategy that improves the robustness of growth estimates and strengthens their applicability in conservation-oriented assessments, especially for data-poor species.

Disk width alone appeared to have low statistical power suggesting that this single morphometric trait may not be sufficient to detect sexual dimorphism. However, growth modelling approaches (both frequentist and Bayesian), which integrate information across age and size, revealed strong and consistent differences between sexes. This highlights the importance of using model-based approaches rather than relying on single summary metrics when assessing dimorphism in data-limited contexts. Therefore, growth results obtained in this study revealed clear sexual dimorphism in growth parameters as demonstrated by the likelihood test on frequentist approach and further supported by the comparison of Bayesian posterior distribution between sexes, both based on the entire sample. Considering the entire sample, females exhibited the highest estimated asymptotic length ($DW_{\infty} = 872.94$ mm) but also the lowest growth rate ($k = 0.11$). In contrast, males appeared to be capable of attaining much smaller asymptotic lengths ($DW_{\infty} = 511.11$ mm), yet showed a much higher growth rate ($k = 0.36$). A similar pattern was observed in Sardinia, though with slightly lower DW_{∞} values for both sexes (females = 758.66 mm; males = 658.20 mm) with growth rates equals to 0.16 and 0.24, respectively for females and males. However, as mentioned above, the absence of larger specimens could have contributed to these discrepancies between the Sardinian and the entire sample, with the latter benefiting the presence of the larger Sicilian specimens. Nonetheless, these results seem to suggest the presence of a strong sexual dimorphism in the common eagle ray as typically observed in other batoid species, where females tend to grow more slowly but reach larger sizes, presumably due to reproductive needs such as accommodating developing embryos (Sulikowski et al., 2007; Mulas et al., 2015; Barnett et al., 2013). To our knowledge, only Özten et al. (2024) have previously analysed the growth of *M. aquila*, based on specimens from the Gulf of Saros (northeastern Mediterranean). This study hypothesised a longer lifespan for the species, reporting observations of specimens that were estimated to be up to 10 and 16 years old for males and females, respectively. In this regard,

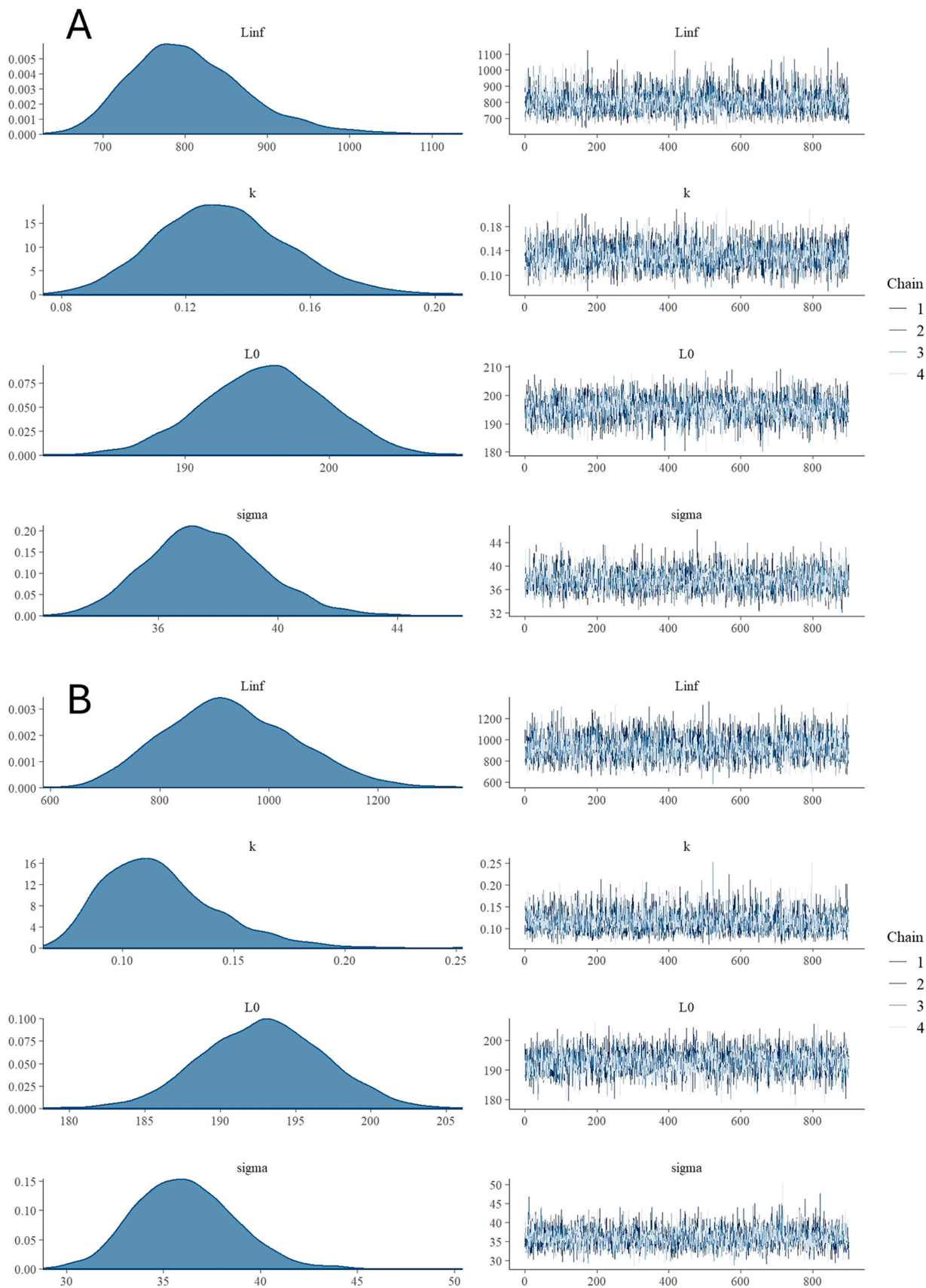


Fig. 7. MCMC chain convergence of the best fitting model (von Bertalanffy) for the entire sample (A), Sardinian sample (B) and Sicilian sample (C) of *Myliobatis aquila*.

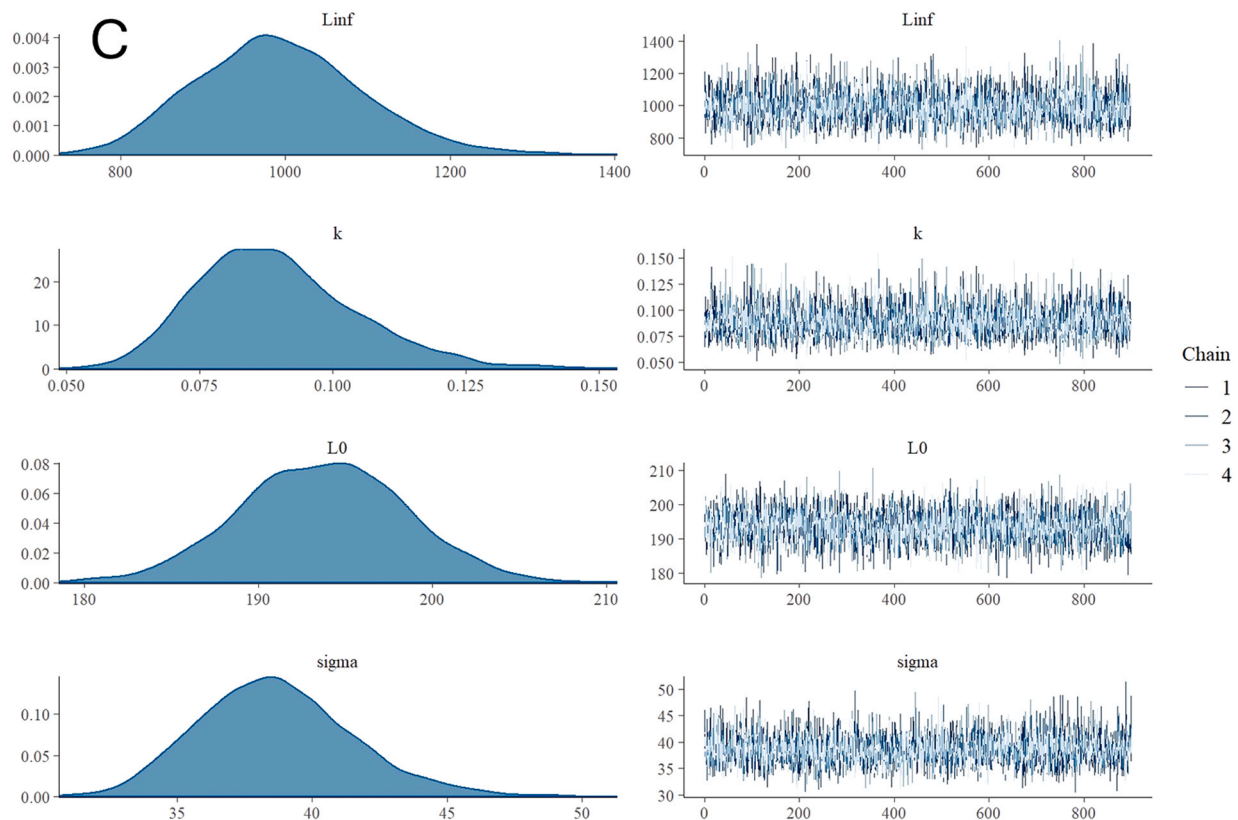


Fig. 7. (continued).

common eagle rays seem to be able to grow older in Turkish waters compared to what was observed in the present study (6–10 years). Additionally, in Turkish waters (Özten et al., 2024) the common eagle ray was estimated to grow larger than suggested in our analysis, and also exhibiting a higher growth rate ($k = 0.90 \text{ y}^{-1}$ for males; $k = 0.95 \text{ y}^{-1}$ for females) compared both to what observed in our study for this species and in general for batoids (e.g. Liu et al., 2021). These discrepancies could be due to differences in both environmental and human-driven conditions that may characterise the two studied areas. It is well established that elasmobranch growth can vary considerably in response to environmental factors such as temperature, salinity, primary productivity, and prey availability (Wetherbee et al., 2012; Mulas et al., 2019). Moreover, anthropogenic pressure and pollution can impair metabolism and reduce somatic growth potential (Aranha et al., 2009; Bellodi et al., 2021; Carbonara et al., 2022). While it represents an important contribution, the analysis from Özten et al. (2024) refers to a geographically distant population subject to different environmental conditions, thus highlighting the need to investigate local growth dynamics, particularly in other Mediterranean areas. An additional source of uncertainty in age estimation arises from age-reading variability, which can stem from both biological and methodological factors. These findings highlight how aspects such as preparation technique, vertebral clarity, and reader interpretation can influence ageing outcomes (Bellodi et al., 2024). Moreover, reader experience has been shown to play a critical role in minimizing variability, with trained and consistently calibrated readers achieving higher reproducibility in annulus counts (Carbonara et al., 2019; Campana, 2014). In the present study, the strong agreement between independent readers suggests a high level of competence and consistency; however, given the observed variability reported in comparable research, the influence of reader expertise and interpretative subjectivity cannot be completely excluded. Recognizing this factor is essential for ensuring that inter-study comparisons and growth parameter estimations are based on harmonized and validated

ageing protocols.

Integrating environmental, ecological, and anthropogenic factors into future studies could enhance our understanding on the geographic variability observed in growth parameters. Given that *M. aquila* is currently considered heavily threatened (Malak et al., 2011; Jabado et al., 2021)), the data provided by this study represent a crucial step toward the development of effective management strategies. The confirmation of slow female growth and the long time required to reach maximum sizes underscores the urgency of including this species in stricter management plans, both for trawl and artisanal fisheries.

A notable limitation of this study is the sample representativeness, particularly in Sicily, where the absence of small-sized individuals required the exclusive use of back-calculated data. Despite this constraint, the combined dataset offers the first regional-scale assessment of *M. aquila* growth in the central-western Mediterranean. Moreover, to fully interpret the results presented in this study, it is important to consider the constraints under which samples were collected. In fact, the present study focuses on a rare species, for which sampling opportunities are inherently limited, and ethical considerations necessarily restrict the collection of biological material. In this regard, our sampling was necessarily constrained to individuals found dead in order to minimize impacts on this threatened species. As expected, sampling effort was temporally uneven and concentrated during summer months, reflecting both field logistics (e.g. MEDITS survey protocol) and seasonal variability in detectability. Moreover, DW varied significantly across areas and months, indicating spatial and seasonal heterogeneity in size structure. While these patterns may influence growth estimates, bootstrap sensitivity analyses demonstrated that central disk width estimates were robust. In fact, despite the significant seasonal bias in sampling detected, sensitivity analyses demonstrated that the exclusion of summer samples did not substantially alter DW estimates. This suggests that, in spite of the uneven temporal coverage, the overall size structure of the dataset appeared robust. Nonetheless, seasonal differences in size

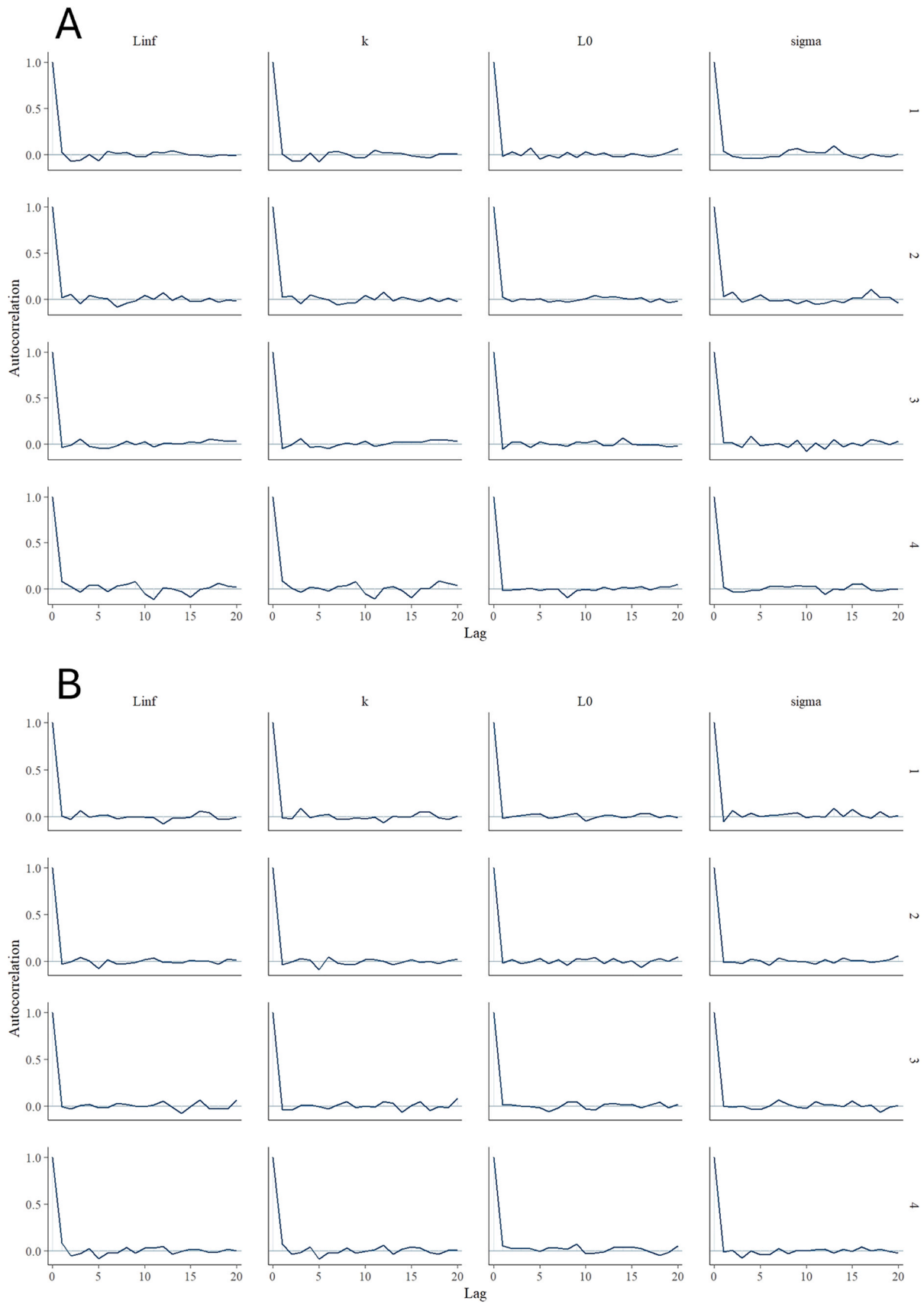


Fig. 8. MCMC Growth parameters autocorrelation from best fitting model (von Bertalanffy) for the entire sample (A), Sardinian sample (B) and Sicilian sample (C) of *Myliobatis aquila*.

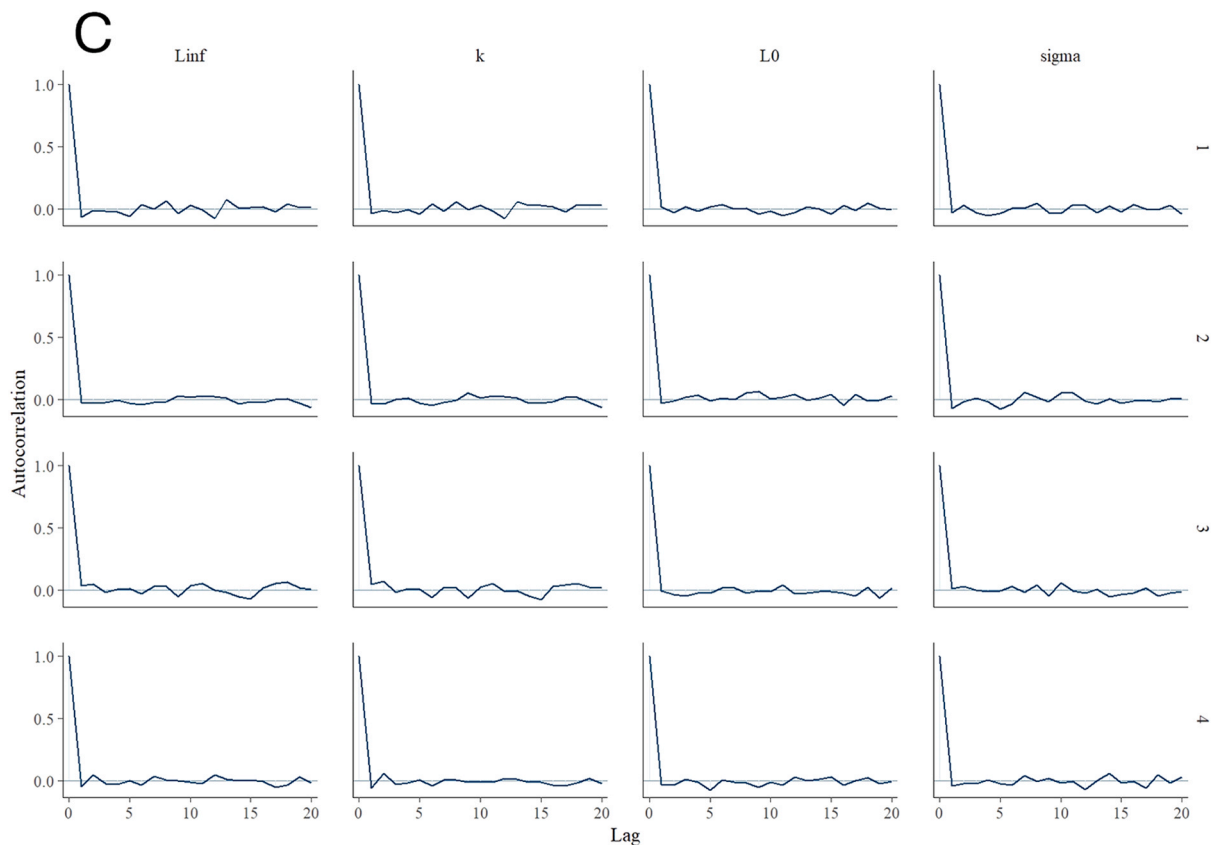


Fig. 8. (continued).

distribution were still evident, indicating that specific life stages may be unevenly represented. Such biases should therefore be considered when interpreting growth-related patterns and potential implications for population vulnerability. Therefore, future monitoring efforts should aim to balance temporal coverage and incorporate non-lethal morphometric data from live individuals to reduce potential bias.

The growth parameters estimated in this study indicate the common eagle ray as a species characterised by a relatively slow life-history strategy, particularly in females. This could suggest a high vulnerability to fishing pressure, especially if large individuals are selectively removed, being more easily caught by artisanal gears (e.g. trammel nets). The Bayesian framework further strengthens these implications by explicitly accounting for uncertainty in growth estimates, supporting the adoption of precautionary management approaches in data-limited contexts (Smart and Grammer, 2021). Therefore, management actions, besides supporting a general no-retention policy, should prioritise the protection of both large reproductive individuals and smaller size classes, eventually allowing them to reach the size at first maturity. In this regard, future studies aimed at comprehensive assessments of maturity and reproductive biology appear essential to finally support the definition of minimum conservation reference sizes (MCRS) for this species.

In conclusion, this study, conducted on populations of *Myliobatis aquila* in the Western-Central Mediterranean, has provided new and valuable insights into the growth pattern of a species which has often been considered poorly documented in the region; therefore, the present study could represent a solid step toward a better knowledge of this ecologically important and threatened species. Considering the incidental nature of the capture of this rare batoid species, the implementation of effective management measures within the target fishery remains challenging. Nevertheless, robust data on the species' life history traits and, particularly, on its growth patterns, could contribute significantly to understanding the vulnerability degree of the common eagle ray. Such information could support comprehensive risk

assessment analyses, eventually leading to a more conscious handling of this bycatch species.

Funding

This research did not receive any specific grant from funding agencies in the public, commercial, or not-for-profit sectors.

CRedit authorship contribution statement

Pierluigi Carbonara: Writing – review & editing, Investigation, Formal analysis. **Blondine Agus:** Writing – review & editing, Investigation. **Mauro Sinopoli:** Writing – review & editing, Supervision, Project administration, Funding acquisition. **Massimiliano Bottaro:** Supervision, Project administration, Funding acquisition. **Maria Cristina Follesa:** Writing – review & editing, Supervision, Resources, Project administration. **Andrea Bellodi:** Writing – review & editing, Writing – original draft, Visualization, Validation, Software, Resources, Methodology, Investigation, Formal analysis, Data curation, Conceptualization. **Manfredi Madia:** Writing – review & editing, Writing – original draft, Visualization, Validation, Software, Methodology, Investigation, Formal analysis, Data curation, Conceptualization.

Declaration of Competing Interest

The authors declare that they have no known competing financial interests or personal relationships that could have appeared to influence the work reported in this paper.

Acknowledgments

The authors are grateful to Martina Mazzetti, Maria Rita Amico and Andrea Li Vorsi for the support during the sample collection.

Conflict of interest

The authors declare no conflict of interests.

Appendix A. Supporting information

Supplementary data associated with this article can be found in the online version at [doi:10.1016/j.risma.2026.105029](https://doi.org/10.1016/j.risma.2026.105029).

Data availability

Data will be made available on request.

References

- AAVV, (2017). MEDITS-Handbook, version 9. MEDITS Working Group. Available online at: (<https://www.sibm.it/MEDITS%202011/principaledownload.htm>) (accessed November 2020).
- Akaike, H., 1974. A new look at the statistical model identification. *IEEE Trans. Autom. Control* 19 (6), 716–723. <https://doi.org/10.1109/TAC.1974.1100705>.
- Aranha, A., Menezes, G., Pinho, M.R., 2009. Biological aspects of the velvet belly lantern shark, *Etmopterus spinax* (Linnaeus, 1758) off the Azores, North East Atlantic. *Mar. Biol. Res.* 5 (3), 257–267. <https://doi.org/10.1080/17451000802433175>.
- Barnett, L.A.K., Winton, M.V., Ainsley, S.M., Cailliet, G.M., Ebert, D.A., 2013. Comparative demography of skates: life-history correlates of productivity and implications for management. *PLoS ONE* 8 (5), e65000. <https://doi.org/10.1371/journal.pone.0065000>.
- Beamish, R.J., Fournier, D.A., 1981. A method for comparing the precision of a set of age determinations. *Can. J. Fish. Aquat. Sci.* 38 (8), 982–983. <https://doi.org/10.1139/f81-132>.
- Bellodi, A., Carbonara, P., MacKenzie, K.M., Agus, B., Bekaert, K., Greenway, E.S.I., Follesa, M.C., Madaia, M., Massaro, A., Palmisano, M., Romano, C., Sinopoli, M., Ferragut-Perello, F., Mahé, K., 2024. Measurement of the growth of the main commercial rays (*Raja clavata*, *Raja brachyura*, *Torpedo marmorata*, *Dipturus oxyrinchus*) in European Waters Using Intercalibration Methods. *Biology* 13 (1), 20. <https://doi.org/10.3390/biology13010020>.
- Bellodi, A., Massaro, A., Zupa, W., Donnalioia, M., Follesa, M.C., Ligas, A., Mulas, A., Palmisano, M., Carbonara, P., 2022. Assessing thornback ray growth pattern in different areas of Western-Central Mediterranean Sea through a multi-model inference analysis. *J. Sea Res.* 179, 102141. <https://doi.org/10.1016/j.seares.2021.102141>.
- Bellodi, A., Mulas, A., Carbonara, P., Cau, A., Cuccu, D., Marongiu, M.F., Mura, V., Pesci, P., Zupa, W., Porcu, C., Follesa, M.C., 2021. New insights into life-history traits of Mediterranean electric rays (Torpediniformes: Torpedinidae) as a contribution to their conservation. *Zoology* 146, 125922. <https://doi.org/10.1016/j.zool.2021.125922>.
- Bellodi, A., Mulas, A., Cau, A., Sion, L., Carbonara, P., Follesa, M.C., 2019. Cartilaginous species. In: Carbonara, P., Follesa, M.C. (Eds.), *Handbook on Fish Age Determination: A Mediterranean Experience. Studies and Reviews No. 98*. FAO, Rome, pp. 87–109.
- Bellodi, A., Porcu, C., Cannas, R., Cau, A.L., Marongiu, M.F., Mulas, A., et al., 2017b. Life-history traits of the longnosed skate *Dipturus oxyrinchus*. *J. Fish. Biol.* 90, 867–888. <https://doi.org/10.1111/jfb.13205>.
- Bengil, E.G.T., Başusta, N., (2018). Chondrichthyan species as by-catch: a review on species inhabiting Turkish waters. *J. Black Sea/Mediterr. Environ.* 24 (3), 288–305.
- Bonanomi, S., Pulcinella, J., Fortuna, C.M., Moro, F., Sala, A., 2018a. Elasmobranch bycatch in the Italian Adriatic pelagic trawl fishery. *PLoS One* 13 (1), e0191647. <https://doi.org/10.1371/journal.pone.0191647>.
- Burnham, K.P., Anderson, D.R., 2002. *Model Selection and Multi-Model Inference: A Practical Information-theoretic Approach*, 2nd edn. Springer-Verlag, New York.
- Cabbar, K., Yiğit, C.Ç., 2021. Length–weight relationships of elasmobranch species From Gökçeada Island in the Northern Aegean Sea. *Thalassas* 37, 497–504. <https://doi.org/10.1007/s41208021-00350-z>.
- Campana, S.E., 2014. Age Determination of elasmobranchs, with special reference to Mediterranean species: a technical manual. In: *Studies and Reviews N. 94*. FAO, Rome, p. 38.
- Campana, S.E., 2014. Age determination of elasmobranchs, with special reference to Mediterranean species: a technical manual. *FAO Fish. Aquac. Tech. Paper No. 544*.
- Capapé, C., Guélorget, O., Vergne, Y., Quignard, J.P., 2007. Reproductive biology of the common eagle ray, *Myliobatis aquila* (Chondrichthyes: Myliobatidae) from the coast of Languedoc (Southern France, northern Mediterranean). *Vie Et Milieu / Life & Environ.* 125–130.
- Carbonara, P., Bellodi, A., Palmisano, M., Mulas, A., Porcu, C., Zupa, W., Donnalioia, M., Carlucci, R., Sion, L., Follesa, M.C., 2020. Growth and Age Validation of the Thornback Ray (*Raja clavata* Linnaeus, 1758) in the South Adriatic Sea (Central Mediterranean). *Front. Mar. Sci.* 7, 586094. <https://doi.org/10.3389/fmars.2020.586094>.
- Carbonara, P., Ciccolella, A., De Franco, F., Palmisano, M., Bellodi, A., Lembo, G., et al., 2022. Does fish growth respond to fishing restrictions within Marine protected areas? A case study of the striped red mullet in the south-west Adriatic Sea (central Mediterranean). *Aquat. Conserv. Mar. Freshw. Ecosyst.* 32 (3), 417–429. <https://doi.org/10.1002/aqc.3776>.
- Carbonara, P., Follesa, M.C., 2019. *Handbook on fish age determination: a mediterranean experience. Studies and Reviews*. FAO, Rome, p. 192.
- Carbonara, P., Intini, S., Kolitari, J., et al., 2018. A holistic approach to the age validation of *Mullus barbatus* L., 1758 in the Southern Adriatic Sea (Central Mediterranean). *Sci. Rep.* 8, 13219. <https://doi.org/10.1038/s41598-018-30872-1>.
- Carbonara P., Zupa W., Anastasopoulou A., Bellodi A., Bitetto I., Charilaou C., Chatzisyrou A., Elleboode R., Esteban A., Follesa M.C., Isajlovic I., Jadaud A., García-Ruiz C., Giannakaki A., Guijarro B., Elias Kiparissis S., Ligas A., Mahé K., Massaro A., Medvesek D., Mytilineou C., Ordines F., Pesci P., Porcu C., Peristeraki P., Thasitis I., Torres P., Spedicato M.T., Tursi A., Sion L. Explorative analysis on red mullet (*Mullus barbatus*) ageing data variability in the Mediterranean. *Sci. mar.* <https://doi.org/10.3989/scimar.04999.19A>.
- Carpentieri, P., Nastasi, A., Sessa, M., Srour, A. (Eds.), 2021. *Incidental catch of vulnerable species in Mediterranean and Black Sea fisheries – A review. Studies and Reviews, 101. General Fisheries Commission for the Mediterranean, Rome.*
- Ceyhan, T., Hepkafadar, O., Tosunoglu, Z., 2010. Catch and size selectivity of small-scale fishing gear for the smooth-hound shark *Mustelus mustelus* (Linnaeus, 1758) (chondrichthyes: triakidae) from the Aegean Turkish coast. *Mediterr. Mar. Sci.* 11 (2), 213–223. <https://doi.org/10.12681/mms.73>.
- Champely, S. (2020). *pwr: Basic Functions for Power Analysis*. R package version 1.3.0. CIEM, 2023. *Myliobatis aquila. Mediterranean Marine Species Identification Portal*. Medience Commission (CIEM).
- Colombelli, A., Bonanomi, S., 2022. Length–weight relationships for six elasmobranch species from the Adriatic Sea. *J. Appl. Ichthyol.* 38 (3), 328–332. <https://doi.org/10.1111/jai.14305>.
- Cortés, E., 2002. Incorporating uncertainty into demographic modeling: application to shark populations and their conservation. *Conserv. Biol.* 16 (4), 1048–1062.
- Dulvy, N.K., Pacoureau, N., Rigby, C.L., Pollom, R.A., Jabado, R.W., Ebert, D.A., Fordham, S.V., 2021. Overfishing drives over one-third of all sharks and rays toward a global extinction crisis. *Curr. Biol.* 31 (22), 4773–4787.e8. <https://doi.org/10.1016/j.cub.2021.08.062>.
- Ellis, J.R., McCully Phillips, S.R., Poisson, F., 2017. A review of capture and post-release mortality of elasmobranchs. *J. Fish. Biol.* 90, 653–722. <https://doi.org/10.1111/jfb.13197>.
- Eltink, A.T.G.W. (2000). *Age Reading Comparisons (MS Excel workbook version 1.0 October 2000)*. Available online at: (<http://www.efan.no>) (accessed October, 2000).
- Fabens, A.J., 1965. Properties and fitting of the von Bertalanffy growth curve. *Growth* 29 (3), 265–289.
- Filiz, H., Bilge, G., 2004. Length–weight relationships of 24 fish species from the northern Aegean Sea, Turkey. *J. Appl. Ichthyol.* 20, 431–432. <https://doi.org/10.1111/j.1439-0426.2004.00582.x>.
- Francis, R.I.C.C., 1990. Back-calculation of fish length: a critical review. *J. Fish. Biol.* 36 (6), 883–902. <https://doi.org/10.1111/j.1095-8649.1990.tb05636.x>.
- Gabry, J., Mahr, T. (2025). *bayesplot: Plotting for Bayesian Models*. R package version 1.15.0. (<https://mc-stan.org/bayesplot/>).
- Goldman, K.J., 2006. Age and growth of elasmobranch fishes. In: Musick, J.A., Bonfil, R. (Eds.), *Management Techniques for Elasmobranch Fisheries*, 474. FAO, pp. 97–132 (Fish. Tech. Pap. No).
- Goldman, K.J., Cailliet, G.M., Andrews, A.H., Natanson, L.J., 2012. Assessing the age and growth of chondrichthyan species. In: Carrier, J.C., Musick, J.A., Heithaus, M.R. (Eds.), *Biology of Sharks and Their Relatives*, second ed. CRC Press, Boca Raton, FL, pp. 423–453.
- Gül, G., Demirel, N., 2020. Trophic interactions of uncommon batoid species in the Sea of Marmara. *J. Black Sea/Mediterr. Environ.* 26 (3), 294–309.
- Haddon, M., 2001. *Modelling and Quantitative Methods in Fisheries*. Chapman & Hall, London.
- ICES. (2011). *Report of the Workshop of National Age Readings Coordinators (WKNARC)*. ICES CM 2011/ACOM:45.
- Ilkayaz, A.T., Metin, G., Soykan, O., Kinacigil, H.T., 2008. Length–weight relationships of 62 fish species from the central Aegean Sea, Turkey. *J. Appl. Ichthyol.* 24, 699–702. <https://doi.org/10.1111/j.1439-0426.2008.01167.x>.
- Ismen, A., Ozen, A., Altinagac, U., Ozekinci, U., Ayaz, A., 2007. Weight–length relationships of 63 fish species in Saros Bay, Turkey. *J. Appl. Ichthyol.* 23, 707–708. <https://doi.org/10.1111/j.14390426.2007.00872.x>.
- Jabado, R.W., Chartrain, E., Cliff, G., Da Silva, C., Derrick, D., Dia, M., Diop, M., Doherty, P., Leurs, G.H.L., Metcalfe, K., Pacoureau, N., Porrinos, G., Seidu, I., Soares, A., Tamo, A., VanderWright, W.J., Williams, A.B., Winker, H., 2021. *Myliobatis aquila*. IUCN Red. List Threat. Species 2021 <https://dx.doi.org/10.2305/IUCN.UK.2021.1.RLTS.T161569A12450853.en>.
- Jardas, I., Santic, M., Pallaoro, A., 2004. Diet composition of the eagle ray, *Myliobatis aquila* (chondrichthyes: myliobatidae), in the eastern Adriatic Sea. *Cybiu* 28 (4), 372–374.
- Keskin, Ç., Ordines, F., Ates, C., Moranta, J., Massutí, E., 2014. Preliminary evaluation of landings and discards of the Turkish bottom trawl fishery in the northeastern Aegean Sea (eastern Mediterranean). *Sci. Mar.* 78 (2), 213–225. <https://doi.org/10.3989/scimar.03942.30B>.
- Kimura, D.K., 1980. Likelihood methods for the von Bertalanffy growth curve. *Fish. Bull.* 77, 765–776.
- La Mesa, G., Annunziatellis, A., Filidei Jr., E., Fortuna, C.M., 2016. Bycatch of myliobatid rays in the central Mediterranean Sea: the influence of spatiotemporal, environmental, and operational factors as determined by generalized additive modeling. *Mar. Coast. Fish.* 8 (1), 382–394. <https://doi.org/10.1080/19425120.2016.1167795>.
- Last, P., White, W., de Carvalho, M., Séret, B., Stehmann, M., Naylor, G., 2016. *Rays of the World*. CSIRO Publishing, Clayton.

- Lipej, L., Battistella, R., Mavrić, B., Ivajnsić, D., 2025. Diet of the Common Eagle Ray, *Myliobatis aquila* (Linnaeus, 1758) in the Northern Adriatic Sea. *Fishes* 10 (7), 311. <https://doi.org/10.3390/fishes10070311>.
- Liu, K.M., Wu, C.B., Joung, S.J., Tsai, W.P., Su, K.Y., 2021. Multi-model approach on growth estimation and association with life history trait for elasmobranchs. *Front. Mar. Sci.* 8, 591692. <https://doi.org/10.3389/fmars.2021.591692>.
- Madia, M., Bottaro, M., Cillari, T., Li Vorsi, A., Castriota, L., Amico, M.R., Bizzarri, S., Maggio, T., Falautano, M., Cristina, M., Di Lauro, I., Trova, F., Perzia, P., D'Ambrà, R., Casola, E., Sinopoli, M., 2024. Reducing artisanal fishery impact on marine community: New data from comparison of innovative and traditional gear. *Fishes* 9 (5), 171. <https://doi.org/10.3390/fishes9050171>.
- Malak, D.A., et al., 2011. Overview of the conservation status of the marine fishes of the Mediterranean Sea. IUCN, Gland, Switzerland, and Malaga, Spain.
- Mazerolle, M.J. (2020). Aicmodavg: Model Selection and Multimodel Inference Based On (Q)Aic(C). R Package Version 2.3-1. Available at: (<https://Github.Com/Cran/Aicmodavg>).
- Mulas, A., Bellodi, A., Cannas, R., Cau, A., Cuccu, D., Marongiu, M.F., Porcu, C., Follesa, M.C., 2015. Diet and feeding behaviour of longnosed skate *Dipturus oxyrinchus*. *J. Fish. Biol.* 86 (1), 121–138. <https://doi.org/10.1111/jfb.12551>.
- Mulas, A., Bellodi, A., Cannas, R., Carbonara, P., Cau, A., Marongiu, M.F., Pesci, P., Porcu, C., Follesa, M.C., 2019. Resource partitioning among sympatric elasmobranchs in the central-western Mediterranean continental shelf. *Mar. Biol.* 166, 153. <https://doi.org/10.1007/s00227-019-3607-0>.
- Natanson, L.J., Kohler, N.E., Ardizzone, D., Cailliet, G.M., Wintner, S.P., Mollet, H.F., 2006. Validated age and growth estimates for the shortfin mako, *Isurus oxyrinchus*, in the North Atlantic Ocean. In: Carlson, J.K., Goldman, K.J. (Eds.), *Special Issue: Age and Growth of Chondrichthyan Fishes: New Methods, Techniques and Analysis, Developments in Environmental Biology of Fishes*, 25. Springer, Dordrecht. https://doi.org/10.1007/978-1-4020-5570-6_16.
- Ogle, D.H., Wheeler, P., Dinno, A. (2019). Fsa: Fisheries Stock Analysis. R Package Version 0.8.25, Available at: (<https://Github.Com/Droglenc/Fsa>).
- Okamura, H., Semba, Y., 2009. A novel statistical method for validating the periodicity of vertebral growth band formation in elasmobranch fishes. *Can. J. Fish. Aquat. Sci.* 66, 771–780.
- Özten, S., Yiğın, C.Ç., İşmen, A., Cabbar, K., 2024. Biological assessment of the common eagle ray *Myliobatis aquila* (Linnaeus, 1758) from the northeastern Mediterranean (Saros Bay). *Türkiye. Acta Biol. Turc* 37 (S4), 1–11.
- Pacoureaux, N., Rigby, C.L., Kyne, P.M., Sherley, R.B., Winker, H., Carlson, J.K., Dulvy, N. K., 2021. Half a century of global decline in oceanic sharks and rays. *Nature* 589 (7843), 567–571. <https://doi.org/10.1038/s41586-020-03173-9>.
- Porcu, C., Bellodi, A., Cau, A., Cannas, R., Marongiu, M.F., Mulas, A., et al., 2020. Uncommon biological patterns of a little known endemic Mediterranean skate, *Raja polyostigma* (Risso, 1810). *Reg. Stud. Mar. Sci.* 34, 1–13. <https://doi.org/10.1016/j.rsma.2020.101065>.
- R Core Team, 2026. R: a language and environment for statistical computing. R Foundation for Statistical Computing, Vienna, Austria. (<https://www.R-project.org/>).
- Rafrafi-Nouira, S., El Kamel-Moutalibi, O., Amor, K.O.B., Amor, M.M.B., Capapé, C., 2017. A case of hermaphroditism in the common eagle ray *Myliobatis aquila* (chondrichthyes: myliobatidae), reported from the Tunisian coast (Central Mediterranean). *Ann. Ser. Hist. Nat.* 27 (1), 43–48.
- Richards, F.J., 1959. A flexible growth function for empirical use (<https://doi.org>). *J. Exp. Bot.* 10, 290–301. <https://doi.org/10.1093/jxb/10.2.290>.
- Serena, F., 2005. FAO species identification guide for fishery purposes. Field identification guide to the sharks and rays of the Mediterranean and Black Sea. Food and Agriculture Organization of the United Nations.
- Smart, J.J., 2023. BayesGrowth Estim. Fish. Growth Using MCMC Anal. (<https://github.com/jonathansmart/BayesGrowth>).
- Smart, J.J., Grammer, G.L., 2021. Modernising fish and shark growth curves with Bayesian length at-age models. *PLoS ONE* 16 (2), e0246734. <https://doi.org/10.1371/journal.pone.0246734>.
- Smart, J.J., Harry, A.V., Tobin, A.J., Simpfendorfer, C.A., 2013. Overcoming the constraints of low sample sizes to produce age and growth data for rare or threatened sharks. *Aquat. Conserv. Mar. Freshw. Ecosyst.* 23, 124–134. <https://doi.org/10.1002/aqc.2274>.
- Spedicato, M.T., Massutí, E., Mérigot, B., Tserpes, G., Jadaud, A., Relini, G., 2019. The MEDITS trawl survey specifications in an ecosystem approach to fishery management. *Sci. Mar.* 83S1, 9–20. <https://doi.org/10.3989/scimar.04915.11X>.
- Stan Development Team (2025). RStan: the R interface to Stan. R package version 2.32.7. (<https://mcstn.org/>).
- Stevens, J.D., Bonfil, R., Dulvy, N.K., Walker, P.A., 2000. The effects of fishing on sharks, rays, and chimaeras (chondrichthyan), and the implications for marine ecosystems (June). *ICES J. Mar. Sci.* 57 (3), 476–494. <https://doi.org/10.1006/jmsc.2000.0724>.
- Sulikowski, J.A., Irvine, S.B., DeValerio, K.C., Carlson, J.K., 2007. Age, growth and maturity of the roundel skate, *Raja texana*, from the Gulf of Mexico, USA. *Mar. Freshw. Res.* 58 (1), 41–53. <https://doi.org/10.1071/MF06048>.
- Sulikowski, James A.; Morin, Michael D.; Suk, Seung H.; and Howell, William Hunting, "Age and growth estimates of the winter skate (*Leucoraja ocellata*) in the western Gulf of Maine" (2003). *Fishery Bulletin*. 3. https://scholars.unh.edu/biosci_facpub/3.
- Vacchi, M., Serena, F., 2010. Checklist of the Italian marine chondrichthyan (Chondrichthyes). *Biol. Mar. Mediterr.* 17 (1), 642–648.
- Valls, M., Quetglas, A., Ordines, F., Moranta, J., 2011. Feeding ecology of demersal elasmobranchs from the shelf and slope off the Balearic Sea (western Mediterranean). *Sci. Mar.* 75, 633–639.
- Vehtari, A., Gabry, J., Magnusson, M., Yao, Y., Bürkner, P., Paananen, T., Gelman, A. (2025). loo: Efficient leave-one-out cross-validation and WAIC for Bayesian models. R package version 2.9.0, (<https://mc-stan.org/loo/>).
- von Bertalanffy, L., 1938. A quantitative theory of organic growth (inquires of growth laws II). *Hum. Biol.* 10, 181–183.
- Wetherbee, B.M., Gruber, S.H., Rosa, R.S., 2012. Trophic ecology of elasmobranchs. In: Carrier, J.C., Musick, J.A., Heithaus, M.R. (Eds.), *Biology of Sharks and Their Relatives*. CRC Press, pp. 567–592.
- White, W.T., Blaber, S.J.M., Craig, J.F., 2012. The current status of elasmobranchs: biology, fisheries and conservation. *J. Fish. Biol.* 80, 897–900. <https://doi.org/10.1111/j.1095-8649.2012.03268.x>.
- Whitehead, P.J.P., Bauchot, M.L., Hureau, J.C., Nielsen, J., Tortonese, E. (Eds.), 1986. *Fishes of the North-eastern Atlantic and the Mediterranean*, 1–3. UNESCO, Paris.
- Winsor, C., 1932. The Gompertz curve as a growth equation. *Proc. Natl. Acad. Sci. U. S. A.* 18, 1–8. <https://doi.org/10.1073/pnas.18.1.1>.
- Yiğın, C.Ç., İşmen, A., 2009. Length–weight relationships for seven rays from Saros Bay (northern Aegean Sea). *J. Appl. Ichthyol.* 25, 106–108. <https://doi.org/10.1111/j.14390426.2008.01161.x>.